Acta Neuropathol (2014) 128:805–820
DOI 10.1007/s00401-014-1343-6

ORIGINAL PAPER

Direct evidence of Parkinson pathology spread from the gastrointestinal tract to the brain in rats

Staffan Holmqvist · Oldriska Chutna · Luc Bousset · Patrick Aldrin-Kirk · Wen Li · Tomas Björklund · Zhan-You Wang · Laurent Roybon · Ronald Melki · Jia-Yi Li

Received: 14 May 2014 / Revised: 20 September 2014 / Accepted: 20 September 2014 / Published online: 9 October 2014

Abstract The cellular hallmarks of Parkinson's disease (PD) are the loss of nigral dopaminergic neurons and the formation of α-synuclein-enriched Lewy bodies and Lewy neurites in the remaining neurons. Based on the topographic distribution of Lewy bodies established after autopsy of brains from PD patients, Braak and coworkers hypothesized that Lewy pathology primes in the enteric nervous system and spreads to the brain, suggesting an active retrograde transport of α-synuclein (the key protein component in Lewy bodies), via the vagal nerve. This hypothesis, however, has not been tested experimentally thus far. Here, we use a human PD brain lysate containing different forms of α-synuclein (monomeric, oligomeric and fibrillar), and recombinant α-synuclein in an in vivo animal model to test this hypothesis. We demonstrate that α-synuclein present in the human PD brain lysate and distinct recombinant α-synuclein forms are transported via the vagal nerve and reach the dorsal motor nucleus of the vagus in the brainstem in a time-dependent manner after injection into the intestinal wall. Using live cell imaging in a differentiated neuroblastoma cell line, we determine that both slow and fast components of axonal transport are involved in the transport of aggregated α-synuclein. In conclusion, we here provide the first experimental evidence that different α-synuclein forms can propagate from the gut to the brain, and that microtubule-associated transport is involved in the translocation of aggregated α-synuclein in neurons.

Keywords Parkinson's disease · Alpha-synuclein · Lewy body · Protein aggregation · Protein propagation

Electronic supplementary material The online version of this article (doi:10.1007/s00401-014-1343-6) contains supplementary material, which is available to authorized users.

S. Holmqvist · O. Chutna · W. Li · J.-Y. Li (✉)
Neural Plasticity and Repair Unit, Department of Experimental Medical Science, Wallenberg Neuroscience Center, Lund University, BMC A10, 22184 Lund, Sweden
e-mail: jia-yi.li@med.lu.se; jiayili@mail.neu.edu.cn

S. Holmqvist · L. Roybon
Cell Stem Cell Laboratory for CNS Disease Modeling, Department of Experimental Medical Science, MultiPark Strategic Research Area and Lund Stem Cell Center, Lund University, BMC A10, 22184 Lund, Sweden

L. Bousset · R. Melki
Laboratoire d'Enzymologie et de Biochimie Structurale, CNRS, Bâtiment 34, Avenue de la Terrasse, 91190 Gif-Sur-Yvette, France

P. Aldrin-Kirk · T. Björklund
Molecular Neuromodulation Unit, Department of Experimental Medical Science, MultiPark Strategic Research Area, Wallenberg Neuroscience Center, Lund University, BMC A10, 22184 Lund, Sweden

Z.-Y. Wang · J.-Y. Li
College of Life and Health Sciences, Institute of Neuroscience, Northeastern University, 110819 Shenyang, China

Introduction

Parkinson's disease (PD) is the most common movement disorder and the second most common neurodegenerative disease after Alzheimer's disease. The neuropathological hallmarks of PD are loss of dopaminergic neurons in the substantia nigra and the presence of cytoplasmic inclusions called Lewy bodies and Lewy neurites in the remaining surviving dopaminergic neurons [25]. A large body of evidence suggests that these neuropathological features are not only restricted to dopaminergic neurons, but are

also widely exhibited in non-dopaminergic systems. The progressive spread of the Lewy pathology, which is characterized by α-synuclein immunoreactive inclusions in cell bodies and neuronal processes, marks the core of neuropathological staging in most cases of PD. The topographic distribution of such α-synuclein-containing inclusions, first appear in the peripheral nervous system (e.g., enteric neurons in the gut), progresses to lower brain regions, such as the dorsal motor nucleus of the vagus (DMV) and to the substantia nigra (where the primary lesion of dopaminergic neurons locates in PD). Eventually inclusions can be detected in the cerebral cortex. These findings give rise to the notion that a neurotropic pathogen would penetrate the gut epithelium and enter axons of the enteric neurons in the myenteric plexus (Auerbach's plexus); these neurons control the activity of gut smooth muscles; and/or axons of the submucosal plexus (Meissner's plexus), which regulates mucosal secretion and blood flow.

Braak and co-workers hypothesized that this pathogen might spread via retrograde transport to different interconnected brain regions [5, 6, 17]. In Braak's observations, Lewy pathology first manifests in enteric neurons of the gut (stage 1) long before it is present in dopaminergic neurons of the midbrain and PD symptoms are evident (stage 3) [7]. The gap between stages 1 and 3 may take many years. From the periphery, the pathology gains access to the lower brainstem via the vagal nerve and then follows an ascending pathway reaching the substantia nigra and subsequently, the cerebral cortex [28, 40]. Thus, the temporal appearance of Lewy pathology in PD strongly suggests long-distance trafficking of a pathogen in neurons from peripheral tissues to the brain.

We, and others, have shown that intra-striatal transplants of fetal ventral mesencephalic progenitors in PD patients develop Lewy pathology a decade after transplantation, suggesting transfer of Lewy pathology from host to the grafted cells [21–23, 29, 30]. Further experimental studies have shown that Lewy pathology can indeed propagate from one cell to another, not only in cultured cells in vitro, but also in brains of animal models of PD [11, 15, 27, 33]. Moreover, recent reports revealed that α-synuclein could spread along the projection tracts after it was directly injected into the brain of α-synuclein transgenic or wildtype mice [31, 32, 43] and Lee et al. [26] elegantly showed deposition of α-synuclein in myenteric neurons after injecting the brain lysate derived from the patient of dementia with Lewy body (DLB), into the stomach wall of A53T transgenic mice. But, to date, experimental evidence is lacking to show whether α-synuclein pathology can propagate from the gut to the brain, as hypothesized by Braak and his colleagues.

Here, we show that α-synuclein from PD patient brain lysate is taken up and transported retrogradely over a long distance via the vagal nerves from the gut to the brain, after being injected into the wall of the gastrointestinal tract. We confirmed these observations using Atto-550-labeled recombinant α-synuclein forms (monomers, oligomers and fibrils). Additionally, we provide evidence suggesting that aggregated α-synuclein is transported by the fast component of microtubule-based axonal transport as well as in the slow component of axonal transport. Taken together, our findings strengthen the hypothesis that PD pathology may originate in the periphery and gradually propagate to the brain, where it eventually leads to PD.

Materials and methods

Animals

Adult wildtype Sprague Dawley rats (approximately 250 g) were purchased from Charles River Laboratories. Animals were kept with food and water ad libitum under a 12-h light/12-h dark cycle. Housing and procedures were conducted in accordance with ethical permit approved by Malmö-Lund Committee for animal research.

Preparation of brain lysates from PD patient

Brain of a neuropathologically confirmed PD case was provided by Dr. Elisabet Englund, the Brain Bank, Lund University Hospital, Sweden. The patient died of acute aspiration and subsequent cardiac arrest due to advanced PD. Fresh substantia nigra was dissected out (20 h post-mortem), immediately frozen and stored in −80 °C freezer until use. Lysates containing aggregated as well as mono- and oligomeric forms of α-synuclein were prepared with the freshly frozen substantia nigra tissue. The tissue was homogenized at 10 % (w/v) in sterile, phosphate-buffered saline (PBS) at 4 °C, vortexed, sonicated 3 × 5 s and centrifuged at 3,000×*g* at 4 °C for 5 min. Supernatants were kept frozen at −80 °C. The solution for injection was prepared by diluting the PD patient's lysate supernatant before use to a final concentration of 3 % (w/v). Different forms of α-synuclein (1 µg/µl) were resuspended in PBS with or without fluorogold (40 µg/ml).

Preparation of recombinant α-synuclein in monomeric, oligomeric, and fibrillar forms

Expression and purification of recombinant α-synuclein

The expression and purification of human wildtype (WT) α-synuclein was performed as previously described [14]. Briefly, the Escherichia coli strain BL21 (DE3) (Stratagene,

La Jolla, CA, USA) were transformed with the expression vector pET3a encoding WT α-synuclein and the bacteria grown in LB medium to an optical density of 0.8. α-Synuclein expression was induced by 0.5 mM IPTG for 3 h, the cells were lyzed by sonication and the cell lysates were clarified by centrifugation at 14,000*g*, for 30 min. α-Synuclein was precipitated by 50 % ammonium sulfate at 4 °C. The solution was spun at 4,000 g, for 30 min at 4 °C and the resulting pellet was resuspended in 10 mM Tris pH 7.5. The solution was loaded onto a DEAE column eluted by a gradient of 0–500 mM NaCl, and the fractions containing α-synuclein (eluted at 200 mM NaCl) were heated to 75 °C for 20 min. The solution was next clarified by centrifugation at 14,000*g*, loaded onto a Superdex 75 HiLoad 26/60 column (GE healthcare), equilibrated and eluted in 50 mM Tris–HCl, pH 7.5, 150 mM KCl. Pure α-synuclein (0.2–0.5 mM) in 50 mM Tris–HCl, pH 7.5, 150 mM KCl was filtered through sterile 0.22-μm filters and stored at −80 °C. α-Synuclein concentration was determined spectrophotometrically using an extinction coefficient of 5,960 M^{-1} cm^{-1} at 280 nm.

Assembly of monomeric α-synuclein into oligomers and fibrils

For oligomer formation, α-synuclein (200 μM) was incubated in buffer A (50 mM Tris–HCl, pH 7.5, 150 mM KCl) at 4 °C, without shaking, for 7 days. Oligomeric α-synuclein was separated from the monomeric form of the protein by size-exclusion chromatography (Superose 6 HR10/300, GE Healthcare). For fibril formation, α-synuclein was incubated in buffer A at 37 °C under continuous shaking in an Eppendorf Thermomixer set at 600 r.p.m. Assembly was monitored continuously in a Cary Eclipse spectrofluorimeter (Varian Inc., Palo Alto, CA, USA) in the presence of Thioflavin T with excitation wavelength set at 440 and emission wavelengths set at 480 and an averaging time of 1 s.

Fluorescent labeling of monomeric, oligomeric and fibrillar α-synuclein assemblies and BSA

Monomeric and oligomeric α-synuclein assemblies in buffer A were buffer exchanged using NAP10 desalting columns (GE Healthcare) to phosphate-buffered saline (PBS) buffer. We performed α-synuclein labeling with Atto-550 NHS ester fluorophore following the manufacturer's instructions (Atto-Tec Gmbh) using a protein:label molar ratio of 1:2 as such two Atto molecules per alpha-synuclein monomer whether monomeric, oligomeric or fibrillar form. The labeling reactions were arrested by addition of 1 mM Tris pH 7.5. We removed unreacted fluorophore using NAP10 desalting columns. For fibrillar α-synuclein labeling, the fibrils were centrifuged twice at 15,000*g* for 10 min, resuspended twice in PBS and labeled as described above. The unreacted fluorophore was removed by a final cycle of two centrifugations at 15,000*g* for 10 min and resuspension of the pelleted fibrils in PBS. Lyophilized BSA was purchased form Sigma (A9418), dissolved in PBS at 5 mg/ml and labeled with ATTO-550 dye using a protein:dye ratio of 1:2 following the same procedure as described for monomeric α-synuclein.

Electron microscopy imaging

The nature of soluble, oligomeric and fibrillar α-synuclein forms was assessed using a JEOL 1400 transmission electron microscope following adsorption onto carbon-coated 200-mesh grids and negative staining with 1 % uranyl acetate. The images were recorded with a Gatan Orius CCD camera (Gatan).

Operation procedures

Animals were anesthetized using isoflurane (2–4 %) and kept at a constant body temperature by the use of a conventional heat pad. A schematic showing how the in vivo experiments were performed is depicted in Fig. 1. For each animal, injections were made using a 10-μl Hamilton syringe into the intestine wall of stomach and duodenum at 5 sites, 1 cm apart. Injections were made in close proximity to the myenteric plexus. Each site was injected with 3 μl of one of the four different forms of α-synuclein (PD brain lysate (2 μg/μl, in total protein content), monomer (1 μg/μl), oligomer (1 μg/μl) or fibril (1 μg/μl), $n = 3$ in each type and each time point). In addition, control animals ($n = 3$) were injected with BSA diluted (1 μg/μl) in phosphate-buffered saline (PBS). Some of the animals were injected with a mixture of the synuclein forms and fluorogold. Following injection, animals were sutured and returned to normal housing conditions.

Tissue collection

After 12 ($n = 15$), 24 h ($n = 15$), 72 h ($n = 15$) and 6 days ($n = 12$) injected animals were anesthetized with sodium pentobarbital and then transcardially perfused with 0.9 % saline followed by fixation using ice-cold 4 % paraformaldehyde (PFA) in PBS. A length of the vagal nerve, ranging from the brainstem to the diaphragm (~80 mm) as well as the brain and segments of the intestine were dissected and post-fixed in 4 % PFA overnight. Tissues were then stored in 0.1 M PBS with 20 % sucrose at 4 °C. Transverse serial sections of the medulla oblongata, 30 μm thick, were cut in a microtome (Leica, SM 2010R). Vagal nerves were

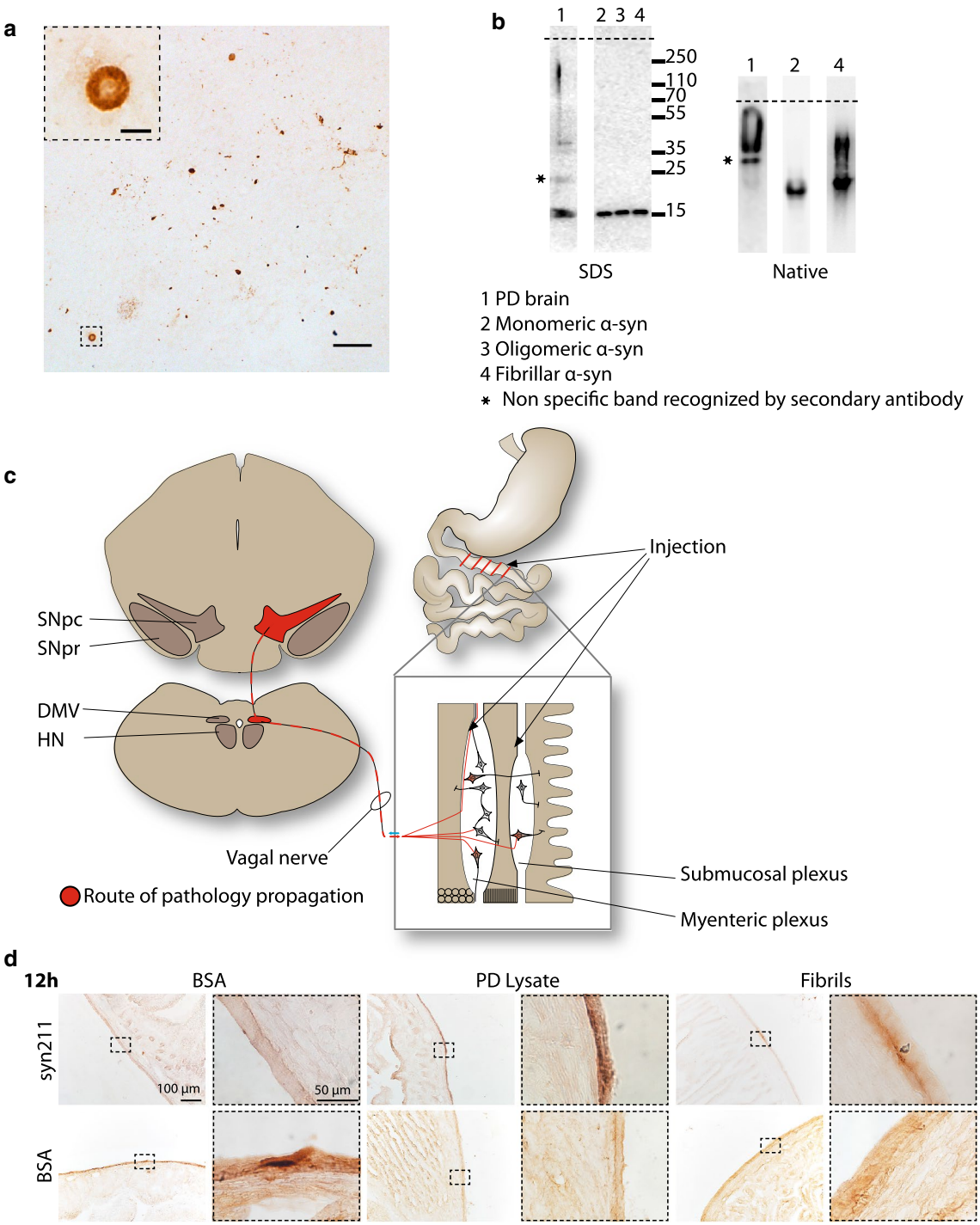

divided into proximal (0–15 mm), medial (25–40 mm) and distal (50–65 mm) segments from the skull base, before entering the CNS. We then made transverse and longitudinal sections, 14 µm, in a cryostat (Leica, CM 3050S) and mounted them on precoated glass slides. Slides were stored at −20 °C before staining. Some sections were immediately separated, mounted on slides, coverslipped with PVA-DABCO and imaged for detection of the fluorescent tags of injected proteins.

Diaminobenzidine (DAB) staining

Freshly frozen tissue from PD patient was fixed with 4 % PFA at room temperature for 10 min. Human brain sections and rat vagal nerve sections were stained on slides and after quenching in 3 % H_2O_2 in pure methanol, incubated with anti-α-synuclein LB 509 (mouse monoclonal, Life Technologies, 1:700), or anti-α-synuclein (mouse monoclonal, Santa Cruz Biotechnology 1:1,000) at 4 °C, overnight.

◀**Fig. 1** Characterization of α-synuclein forms from PD brain lysate and recombinant proteins injected into the intestinal wall. **a** A section of the substantia nigra of the PD patient that the brain lysate for injection was generated from was subjected to immunohistochemistry with an antibody raised specifically against human α-synuclein. The low-power image shows an overview of Lewy pathology (*scale bar* 30 μm). The high-power image (*inset*) shows detail of distinct Lewy body (*scale bar* 10 μm). **b** Western blotting showing components of α-synuclein forms in PD patient brain lysate and monomeric, oligomeric or fibrillar α-synuclein form in SDS-PAGE (8–16 % polyacrylamide gel) or Native PAGE (8–16 % polyacrylamide gel). α-Synuclein shows one band at ~17 kDa in SDS-PAGE. Smear in the Native PAGE indicates the presence of different α-synuclein forms in the brain lysate (*1*) and sonicated synthetic α-synuclein fibrils (*4*). The band labeled with a star corresponds to a protein recognized by the secondary anti-mouse HRP antibody. **c** Overview of the injection sites and pathways interconnecting between the central nervous system and the enteric nervous system. *DMV* dorsal motor nucleus of the vagus, *SNpc* substantia nigra pars compacta, *SNpr* substantia nigra pars reticulata, *HN* hypoglossal nucleus. **d** Immunohistochemical images of the intestines 12 h after injecting BSA (*left*), PD brain lysate (*middle*) and fibrils (*right*) when the sections are immune stained with an α-synuclein antibody (syn211, *upper panels*) or with an antibody against BSA (*low panels*). Distinct α-synuclein immunoreactivities were observed in the PD lysate- or α-synuclein fibril-injected intestines, while distinct BSA immunoreactivity was detected in the BSA-injected intestines. *Scale bars* 100 μm for low-power images, 50 μm for high-power images

Sections were then incubated with a biotinylated anti-mouse secondary antibody (Vector 1:400) at room temperature for 2 h followed by incubation with ABC kit (Vectastain) and DAB kit (Vector laboratories) conventional peroxidase system. Brightfield images were captured on a BX53 Olympus microscope.

Immunofluorescent labeling

We stained transverse sections of medulla oblongata as free-floating on a shaker, while vagal nerve sections were stained mounted on glass slides using a primary antibody specific for human α-synuclein to detect transported α-synuclein. Sections were incubated with the following antibodies: anti-α-synuclein (mouse monoclonal, Santa Cruz 211 1:1,000), anti-choline acetyltransferase (goat, Millipore AB144P 1:500) in combination with secondary antibodies; Alexa-555 anti-mouse (Jackson 1:800), Alexa-488 anti-goat (Jackson 1:800), FITC anti-rabbit (Jackson 1:200). Confocal microscopic images of double-labeled medulla oblongata were captured using a Leica SP8 Scanning confocal microscope using a HyD detector using sequential scanning. Solid-state lasers at wavelengths 488 nm and 552 nm were utilized to excite the respective fluorophores. The pinhole was retained at Airy 1 for all acquisitions. For each acquisition at the same magnification, identical settings were loaded for laser power gain. Post-acquisition, deconvolution was performed using the "Deconvolution" plugin for ImageJ [developed by the Biomedical Imaging Group (BIG), EPFL, Switzerland http://bigwww.epfl.ch/] utilizing the Richardson–Lucy algorithm and applying point-spread functions (PSFs) calculated for the specific imaging equipment using the Gibson and Lanni model in the PSF Generator (BIG, EPFL, Switzerland http://bigwww.epfl.ch/algorithms/psfgenerator/). The same PSF models and deconvolution parameters were applied to all image stacks at the same magnification. Orthogonal projections were generated using ImageJ (v1.48p) without further modifications of the images.

Western blotting

Tissue protein extraction

The substantia nigra of a Parkinson patient (advanced stage) was obtained from Lund Brain Bank, kindly supplied by Dr. Elisabet Englund. The sample was homogenized in the presence of proteases inhibitors using a FastPrep-24 homogenizer (MP Biomedicals, Santa Ana, CA, USA) in a lysis buffer 50 mM Tris/HCl pH 7.4, 150 mM NaCl, 2 mM EDTA, 1 % (v/v) NP-40, 0.1 % (w/v) sodium dodecyl sulfate for further analysis by SDS-PAGE or in lysis buffer 20 mM Tris/HCl pH 7.4, 100 mM NaCl, 0.4 % (w/v) sodium dodecyl sulfate and 0.2 % (v/v) Triton X-100 for Native PAGE. Tissue homogenate was further sonicated twice for 10 s at 30 % amplitude (QSonica, Newtown, CT, USA) with 1-min incubation on ice between each sonication step and centrifuged at 16,000*g* for 15 min at 4 °C. The supernatant was recovered and protein concentration was quantified using BCA protein assay (Thermo Fisher Scientific, Rockford, IL, USA).

SDS-PAGE, native PAGE and Western blotting analysis

Brain extract from a patient developing PD, monomeric, oligomeric and fibrillar α-syn were either mixed with SDS-PAGE loading buffer and heated to 100 °C and analyzed on a 8–16 % polyacrylamide gel or with Native PAGE loading buffer and analyzed on a 8–16 % polyacrylamide. The samples were transferred to nitrocellulose membranes and probed with mouse anti-α-synuclein-1 antibody (S63320 BD Transduction Laboratories 1:1,000 dilution).

Cell culture, transfection and differentiation

Stable human neuroblastoma SH-SY5Y cells (passage 7–10) were maintained in DMEM Glutamax media (Gibco) supplemented with 10 % FBS (Sigma) in a humidified 5 % CO_2 atmosphere at 37 °C. On the first day of the experiment, 20,000 cells were seeded into the center wells of four-well borosilicate glass chamber slides (Nunc) coated with matrigel (BD Bioscience), the

remaining wells were filled with ddH_20 to avoid evaporation. The following day, cells were induced for neuronal differentiation by addition of 10 μM retinoic acid (RA) to the medium. On day four of differentiation, cells were transiently transfected using Lipofectamine 2000 (Life technologies) with plasmids expressing bimolecular fluorescence complementation (BiFC) vectors of truncated (N- or C-terminus), full-length Venus fused to human wildtype α-synuclein [15], Venus alone (kindly provided by Dr. Tiago Outerio, Göttingen, Germany) or Actin-GFP. The following day, media were replaced with fresh media supplemented with 10 μM RA and 50 ng/ml BDNF whereupon differentiation were continued for four additional days.

Live cell imaging, fluorescence recovery after photobleaching (FRAP) experiments and analyses

FRAP was performed using a Zeiss LSM 510 confocal microscope system running 2009 Zen software with 63×/1.4 Oil DIC Plan-apochromat objective and solid-state 488-nm argon laser for excitation and bleaching of fluorophores. Constant temperature at 35–37 °C, humidity and 5 % CO_2 atmosphere was maintained using a heated stage and chamber system (CTI Controller 3700 digital, temp controller 37-2). FRAP was performed based on conventional FRAP procedure with minor modifications [3, 48]. Before each imaging session media were replaced with imaging buffer consisting of HBSS (Life technologies) supplemented with 5 mM glucose, 1.8 mM $CaCl_2$, 1 mM $MgCl_2$ and 20 mM HEPES, pH 7.4. Working at 256 × 256 pixel resolution, pre- and post-bleaching images were collected using 0.8 % laser power to avoid photobleaching and phototoxicity at a rate of 5 Hz with pinhole set to maximum. Each experiment started with the collection of 4 baseline images. Bleaching was then performed with 100 % laser power for 5 iterations within a circular field 100 μm in diameter, covering an area of the neurite located 100–200 μm away from the cell body. Following the photobleach, fluorescence intensities were recorded for 44 s in bleached, cell body reference and background regions. For each group; expressing α-synuclein-BiFC-Venus ($n = 4$), α-synuclein-Venus ($n = 5$), Actin-GFP ($n = 6$) and Venus alone ($n = 5$) three cells were imaged. Values averaged from the three cells in each experiment constitute one n. To investigate whether mobility was dependent on microtubule dynamics, separate experiments were then performed in which 10 nM of vinblastine was added to the media, after 1-h incubation groups α-synuclein-BiFC-Venus ($n = 2$), α-synuclein-Venus ($n = 3$), Actin-GFP ($n = 5$) and Venus alone ($n = 5$) were imaged.

FRAP data analyses

Raw intensity signals were normalized, by subtracting the average background intensity for each time point (Supplementary Equation 1) as well as correcting for acquisition bleaching for each time point by adjusting to loss of fluorescence within the non-bleached reference region (Supplementary Equation 2, Supplementary Equation 3) [39]. Normalized data from each cell were then individually fitted to appropriate models. The type of model used for each protein was chosen to best describe the bleach corrected and normalized intensity data. For this, data from cells in α-synuclein-BiFC-Venus, α-synuclein-Venus and Actin-GFP groups were fitted to an exponential chemical-interaction model as described by Eq. (1) [39] as α-synuclein and actin are known to interact with other proteins. In contrast, vinblastine-treated cells and those expressing Venus alone were fitted to the empirical diffusion model described by Ellenberg's Eq. (3) [12]. From this, the mobile fraction was deduced with correction for gap ratio, Eq. (2). Fittings of FRAP curves that deviated significantly from normalized raw data were excluded from further analysis. All curve fittings and normalizations were performed in Igor Pro v6.32A using the plugin K_FRAPcalc v9 [developed by the European Advanced Light Microscopy Network (EAMNET)—EMBL—Germany http://www.embl.de/eamnet/].

$$I(t) = y_0 + Ae^{-\tau_1 t} \tag{1}$$

(1) Single exponential model according to Phair single exponential, double normalization

$$\text{Mob} = \frac{\left(\frac{-A}{1-(y_0+A)}\right)}{\text{Gap ratio}} \tag{2}$$

(2) For calculation of mobile fraction with correction for gap ratio

$$I(t) = I_{\text{final}}\left(1 - \left(\frac{w^2}{w^2 + 4\pi Dt}\right)^{1/2}\right) \tag{3}$$

(3) Ellenberg's I final will be considered as the mobile fraction.

Statistical analysis

All data were analyzed using GraphPad Prism software (developed by GraphPad Software, San Diego, USA http://www.graphpad.com). FRAP groups were analyzed by one-way ANOVA for difference among the groups, then groups in-between were compared pairwise by student's t test.

Figures and artwork

Vector graphics and schematics were created using Adobe illustrator CS5 and figures arranged and compiled using Adobe InDesign CS5.

Results

α-Synuclein from a PD patient lysate is transported via the vagal nerve from the intestine to the brain

α-Synuclein is an abundant protein in the neuron. In the brain of PD patients, the protein is misfolded and aggregated, forming Lewy bodies and Lewy neurites in dopaminergic neurons of the substantia nigra as well as in other types of neurons in different brain regions. We first collected fresh substantia nigra tissue from a neuropathologically confirmed Parkinsonian case. Immunohistochemical analysis confirmed the presence of distinct α-synuclein-positive Lewy body structures in brain sections (Fig. 1a). This tissue was therefore used for PD brain lysate preparation. Here, we performed biochemical analyses of the brain lysate preparation to assess the different forms of α-synuclein it contained. Under denaturing conditions, in the presence of SDS, α-synuclein appears monomeric with a molecular weight of ~17 kDa (Fig. 1b); while the native PAGE reveals the presence of higher molecular α-synuclein forms in the brain lysate (Fig. 1b).

After confirming the presence of the α-synuclein forms in the lysate, we injected 3 µl of this lysate (2 µg/µl, total protein) into the intestine of wildtype adult rats (Fig. 1c) and assessed the presence of α-synuclein in the vagal nerve by immunohistochemistry using an antibody that specifically recognize human α-synuclein (See: Materials and methods). We detected distinct α-synuclein immunoreactivity in the intestinal wall (Fig. 1d, middle panel) and in the vagal nerve at time-dependent matter (12, 48, and 72 h post-injections) (Figs. 2, 3, middle panels). No human α-synuclein was detected in the controls, which were injected with bovine serum albumin (BSA) (Figs. 1d, 2). When a BSA antibody was used, no distinct immunoreactivity was detected in the vagal nerves at different time points (Supplement Fig. 1).

Together, these experiments demonstrate that the PD brain lysate contains different α-synuclein forms, and they show that α-synuclein from the injected lysate is taken up and transported via the vagal nerve to the brain. In contrast, although BSA is present in the injection site of the intestinal wall, it is not taken up and transported into the vagal nerve.

Different α-synuclein forms are transported from the intestine to the brain via the vagal nerve

We have shown that the brain lysate contains a mixture of monomeric and multimeric α-synuclein forms. However, it is not clear which form(s) of the protein is taken up and transported to the vagal nerve. Thus, we performed the experiments with distinct, characterized α-synuclein forms. These were fluorescently labeled to allow direct visualization; we determined the nature of each α-synuclein form by SDS-PAGE and native PAGE (Fig. 1b) and transmission electron microscopy (Fig. 4a). Size-exclusion chromatography analyses further revealed the defined and size-specific forms of α-synuclein used in the experiments (Fig. 4b).

When aggregated α-synuclein in the form of fibrils was injected, we observed distinct α-synuclein in the intestinal wall (Fig. 1d) and in the vagal nerve at time-dependent manner (Fig. 2), similar to the PD brain lysate. Particularly, in the high-power images, we could clearly see intensely immune-stained nerve fibers of the vagal nerves in the PD brain lysate- and fibril-injected animals (Fig. 3). In order to verify that different forms of α-synuclein are indeed transported from the intestines to the brain, we injected monomeric, oligomeric or fibrillar Atto-550-α-synuclein with fluorogold, (a live dye, used as a control for the injection) into the intestinal wall of the adult rats. Forty-eight hours later, we detected fluorogold and Atto-550 positive fluorescent punctae in neurons in the DMV, for monomeric, oligomeric and fibrillar forms of α-synuclein we injected. Most, if not all, Atto-550-α-synuclein-positive structures overlapped with fluorogold fluorescence (Supplement Fig. 2a–c). When fluorogold was co-injected with unlabeled PD brain lysate, no Atto-550 fluorescence was observed (Supplement Fig. 2d). These data strongly indicate that the human α-synuclein found in the neurons of the DMV was transported from the injected sites within the intestine.

The neurons of the DMV are cholinergic. To further verify that the human α-synuclein in the DMV is transported from the gastrointestinal wall via the vagal nerve, we double-stained brain sections of medulla oblongata with antibodies against the phenotypic cholinergic enzyme, choline acetyltransferase (ChAT) and human α-synuclein. In samples collected 6 days after intestinal injection, nearly all neurons positively stained for human α-synuclein were also positive for ChAT (Fig. 5b–e). In contrast, no α-synuclein immunoreactivity was detected in controls (BSA-injected animals; Fig. 5a). Interestingly, the animals sacrificed 24 h post-injection did not show any human α-synuclein immunoreactivity in ChAT-positive neurons in the DMV region (Supplement Fig. 3). These data further suggest that different α-synuclein forms are transported over a long distance from the intestine to the brain in a time-dependent manner.

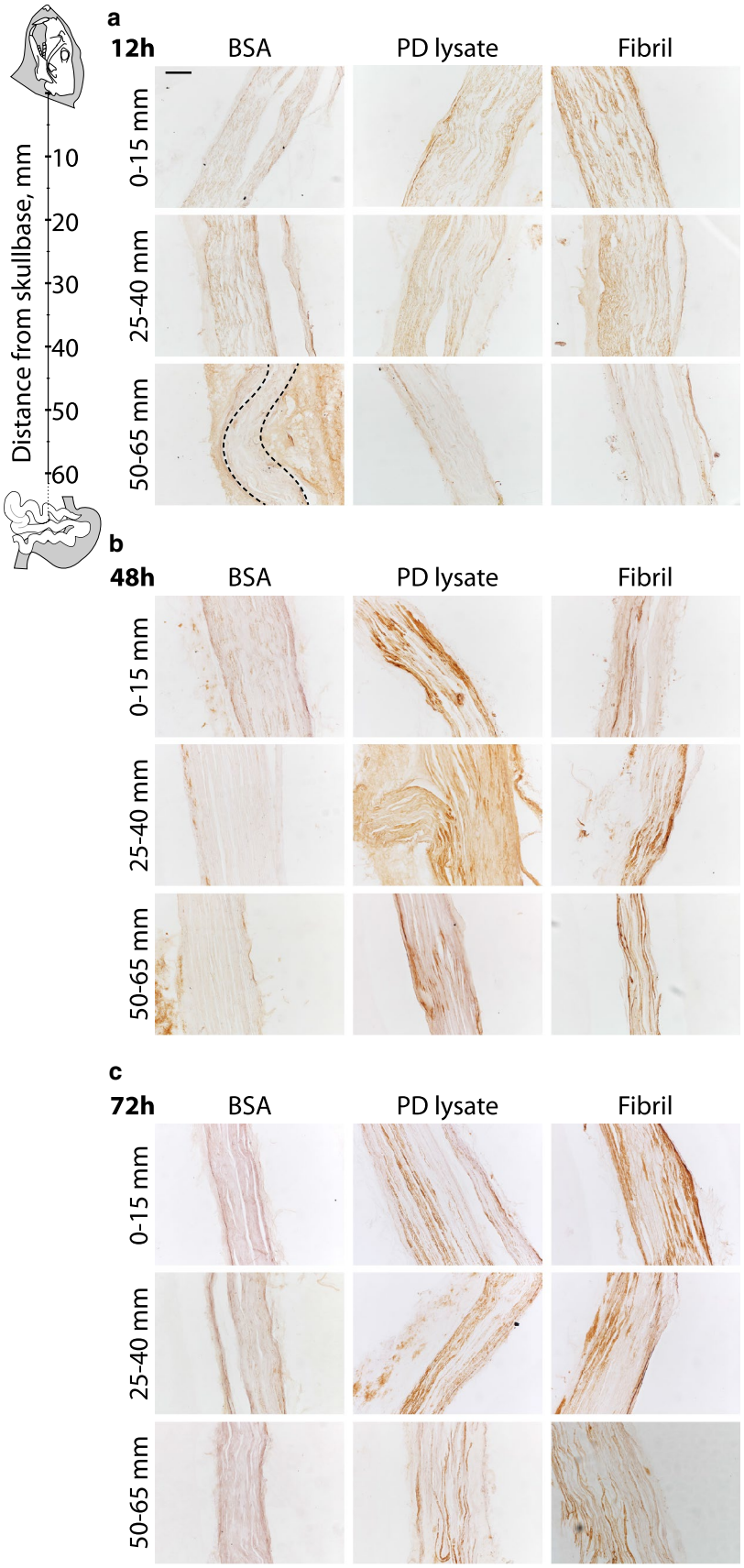

Fig. 2 Time-dependent transport of α-synuclein in the vagal nerve. Schematic drawing on the left illustrating the vagal nerve segments dissected between the skull base and the level of the diaphragm. The actual levels of the segments are shown on the right. Rats received injections of BSA (*left*), PD lysate (*middle*) or α-synuclein fibrils (*right*). The sections of vagal nerves were immunostained with an antibody against human α-synuclein. **a** 12 h after the injection, no distinct α-synuclein immunoreactivity was observed in segments of the vagal nerves from PD lysate- or α-synuclein fibril-injected rats. **b** 48 h after injections distinct α-synuclein immunoreactivity was observed in nerve fibers of the vagal nerves from PD lysate- or α-synuclein fibril-injected rats, in contrast to the vagal nerve injected with BSA in the intestines. **c** 72 h after injections, (similar to **b**), distinct α-synuclein immunoreactivity was observed in nerve fibers of the vagal nerves from PD lysate- or α-synuclein fibril-injected rats. *Scale bars* 50 μm

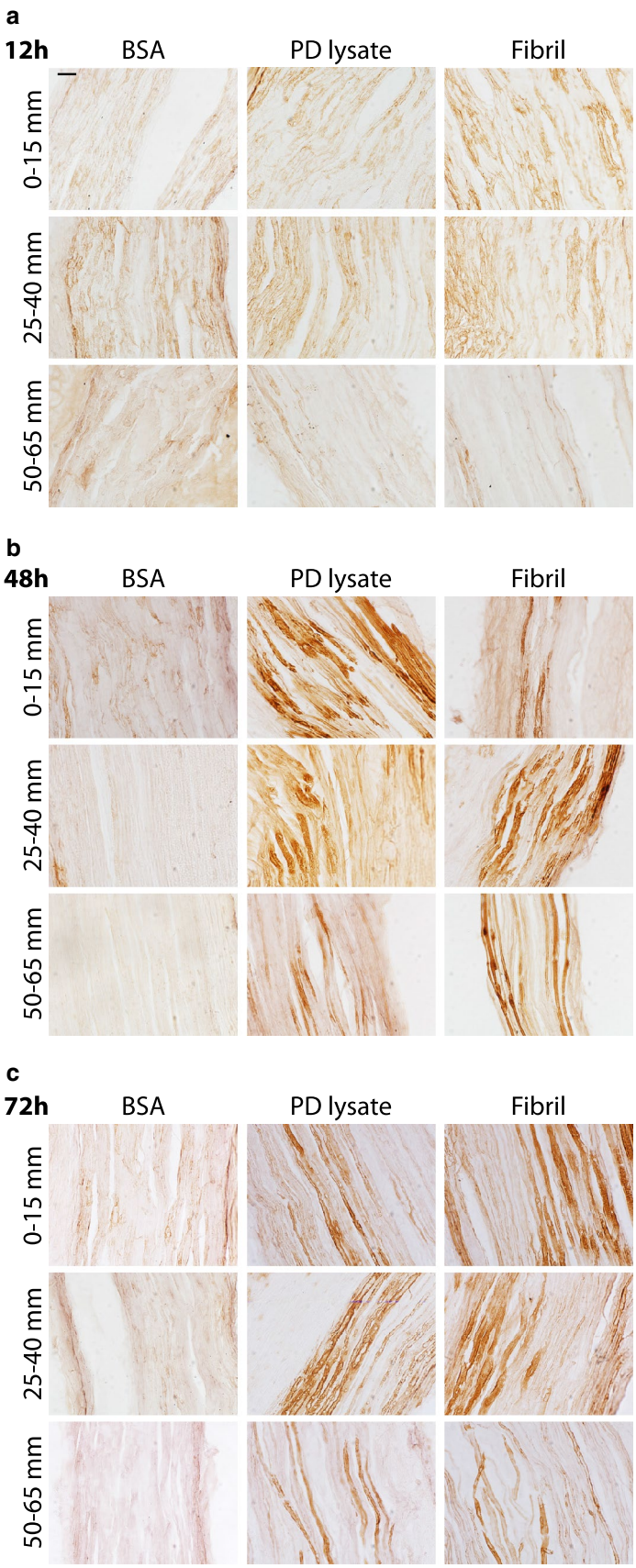

Fig. 3 High-power images of α-synuclein immunoreactivity in sections of vagus nerve 12 h (**a**), 48 h (**b**) and 72 h (**c**) after the injection. Rats received injections of BSA (*left*), PD lysate (*middle*) or α-synuclein fibrils (*right*). **a** No distinct α-synuclein immunoreactivity was observed in segments of the vagal nerves from PD lysate- or α-synuclein fibril-injected rats, 12 h after the injection. **b** Distinct α-synuclein immunoreactivity was observed in nerve fibers of the vagal nerves from PD lysate- or α-synuclein fibril-injected rats, in contrast to the vagal nerve injected with BSA in the intestines, 48 h after injections. **c** Similar to **b**, distinct α-synuclein immunoreactivity was observed in nerve fibers of the vagal nerves from PD lysate- or α-synuclein fibril-injected rats, 72 h after injections. *Scale bar* 20 µm

Transport pattern of aggregating α-synuclein

α-Synuclein is a soluble, unfolded protein, which forms α-helical structures when membrane bound. Previously, we demonstrated that the majority of soluble α-synuclein is located within the cytosol and transports via slow axonal transport, including slow component a (SCa) and slow component b (SCb), while a small fraction (about one quarter) of the total cellular α-synuclein is membrane associated and transports through fast axonal transport, i.e., the fast component [19]. Membrane-bound α-synuclein is α-helical and does not contribute to aggregation and fibrillation, while the soluble form of the protein populates folding intermediates that oligomerize and assemble into fibrils. Our in vivo experiments show that monomeric, oligomeric and fibrillar forms of α-synuclein

Fig. 5 Atto-550-α-synuclein forms specifically transported into the DMV, 144 h after injection into the wall of the intestine. To enhance the signal the brain sections were immunostained with antibodies directed specifically against human α-synuclein (Syn211, *red*, **a**–**e**, **a**″–″, **a**‴–**e**‴) and ChAT (*green*, **da**–**e**, **a**′–**d**′, **a**‴–**e**‴), the phenotypic markers of the DMV. Monomeric (**b**), oligomeric (**c**), fibrillar (**d**) α-synuclein and PD patient brain lysate (**e**) injected animals display double-labeled neurons (*arrows*), while BSA injection does not yield any α-synuclein-positive neurons (a″). *Scale bars* 25 μm in **a**–**e**, and 10 μm in **a**‴–**e**‴ ▶

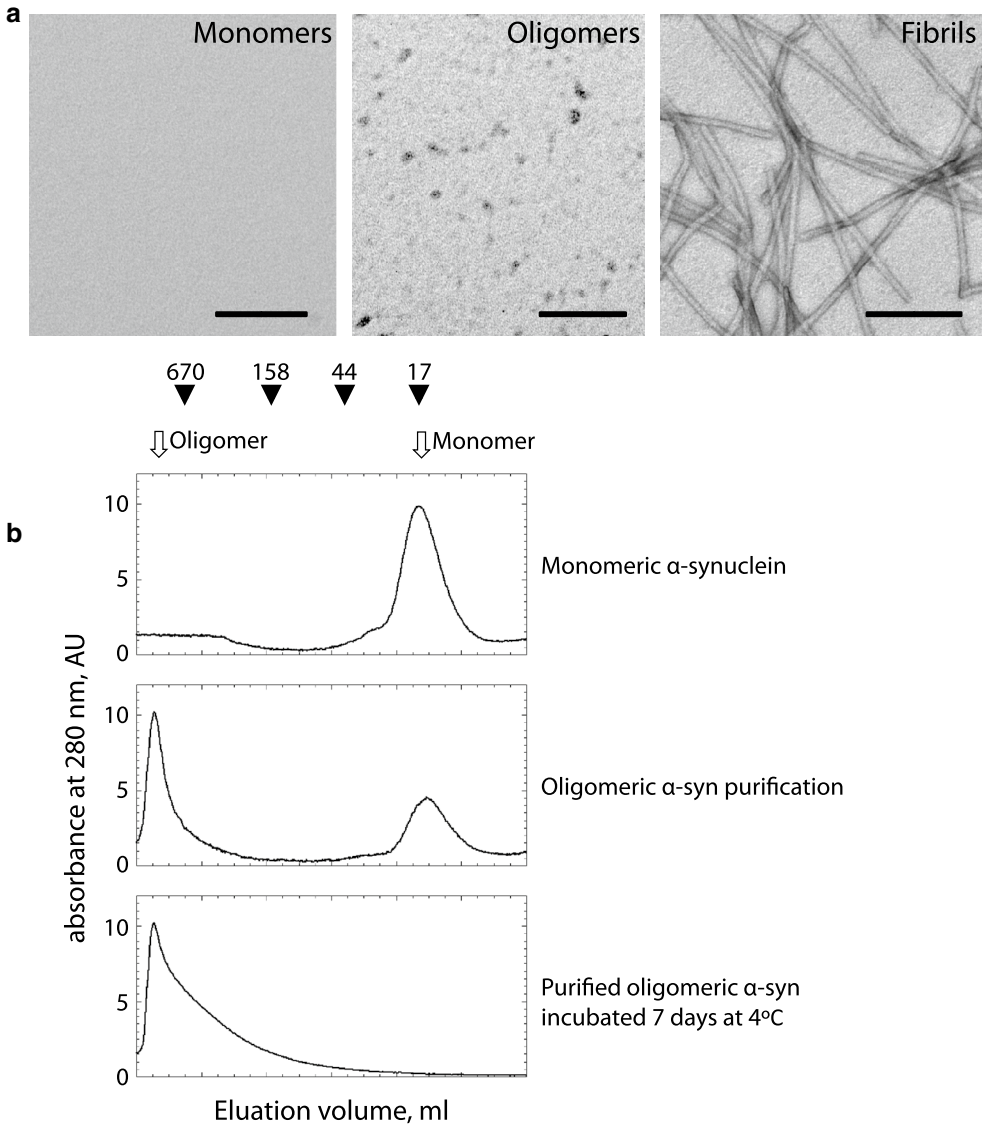

Fig. 4 Characterization of α-synuclein forms. **a** Negatively stained transmission electron micrographs of monomeric, oligomeric and fibrillar α-synuclein. (*Scale bar* represents 200 nm). **b** Size-exclusion chromatography analysis of monomeric and oligomeric α-synuclein. Elution profile of pure recombinant monomeric (*top*) oligomerized α-synuclein (*middle*) and oligomeric α-synuclein incubated 7 days at 4 °C, from a Superose 6 (HR 10/30) column (*bottom*). *Arrows* show the location of oligomeric and monomeric α-synuclein. *Solid arrowheads* show the location of molecular size markers (thyroglobulin 670 kDa; immunoglobulin G 158 kDa; ovalbumin 44 kDa and myoglobin 17 kDa) run under identical conditions on the same column

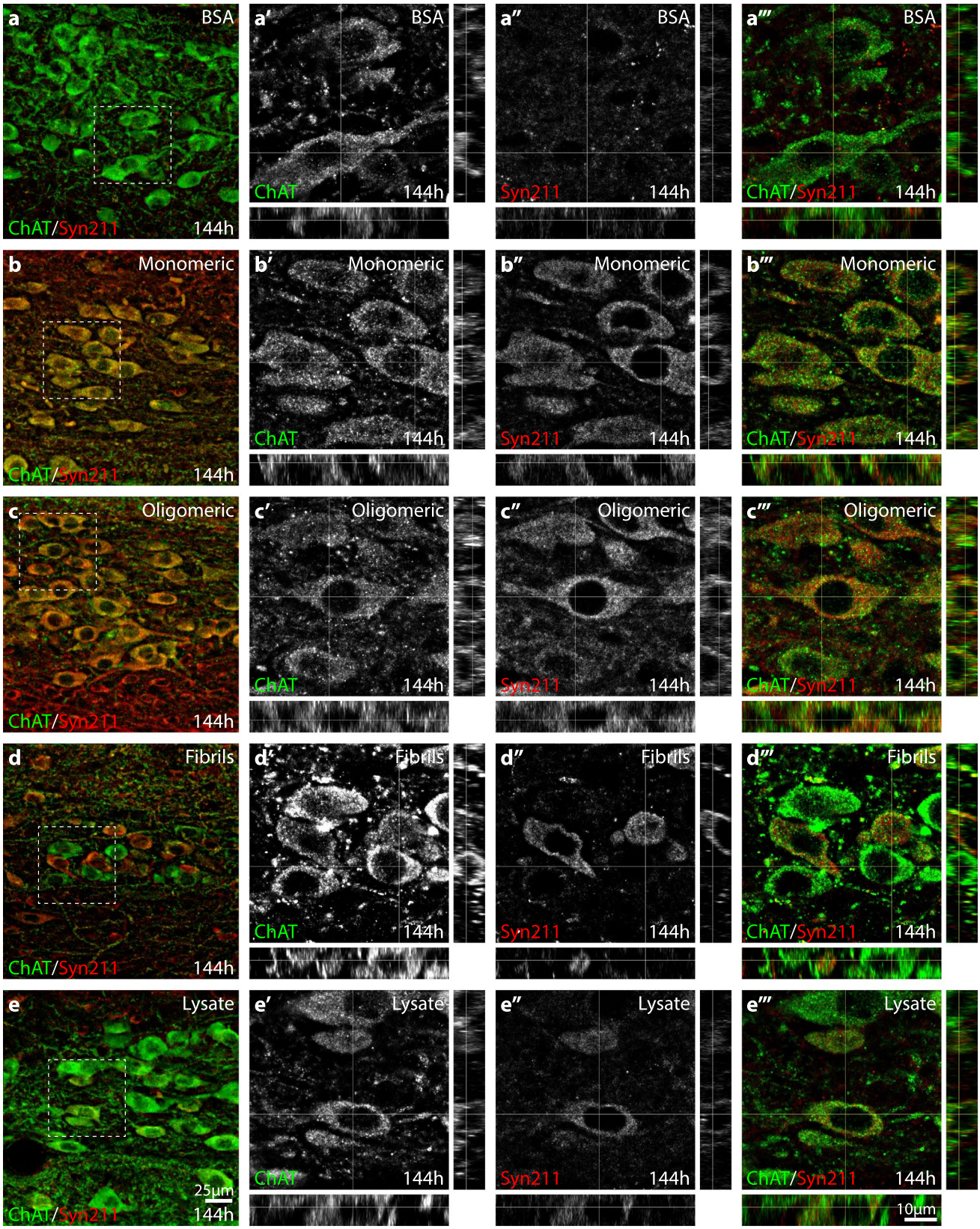
a
BSA
ChAT/Syn211
144h
a′
BSA
ChAT
144h
a″
BSA
Syn211
144h
a‴
BSA
ChAT/Syn211
144h
b
Monomeric
ChAT/Syn211
144h
b′
Monomeric
ChAT
144h
b″
Monomeric
Syn211
144h
b‴
Monomeric
ChAT/Syn211
144h
c
Oligomeric
ChAT/Syn211
144h
c′
Oligomeric
ChAT
144h
c″
Oligomeric
Syn211
144h
c‴
Oligomeric
ChAT/Syn211
144h
d
Fibrils
ChAT/Syn211
144h
d′
Fibrils
ChAT
144h
d″
Fibrils
Syn211
144h
d‴
Fibrils
ChAT/Syn211
144h
e
Lysate
25µm
ChAT/Syn211
144h
e′
Lysate
ChAT
144h
e″
Lysate
Syn211
144h
e‴
Lysate
ChAT/Syn211
144h
10µm

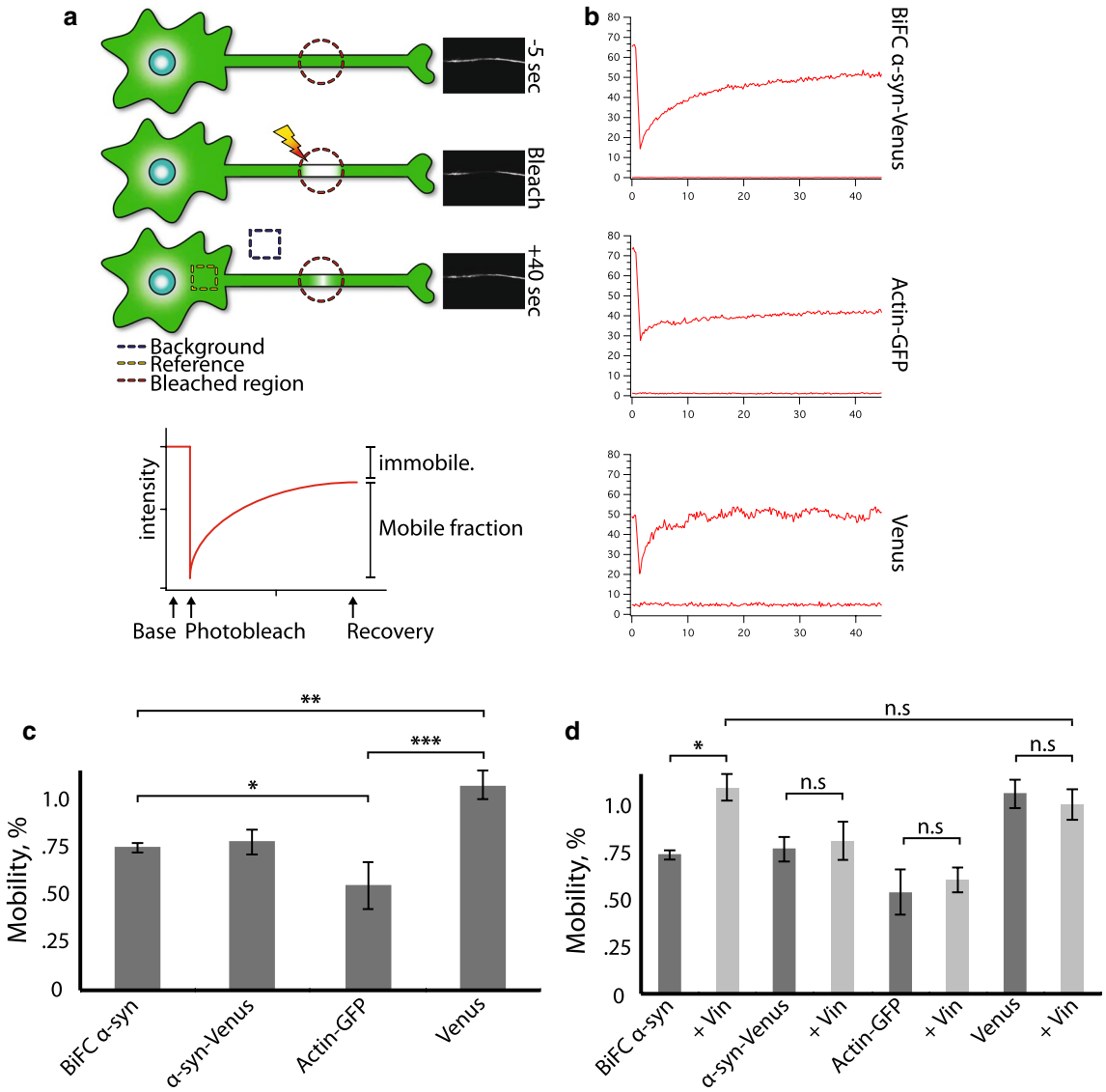

Fig. 6 Mechanisms of transport of α-synuclein assemblies. **a** A schematic drawing showing how the FRAP experiment was performed. To the right representative images of neurite before, during and after fluorescent recovery. **b** Raw, unfitted, FRAP curves for three representative cells expressing complemented α-synuclein-BiFC-Venus, actin-GFP or Venus alone. **c** Normalized and summarized data from fitted curves for mobility of complemented α-synuclein-BiFC-Venus, α-synuclein-Venus, actin-GFP or Venus alone. **d** Data for mobility of same with treatment with 10 nM vinblastine. *$p < 0.05$; $p < 0.0002$; $p < 0.0001$

are retrogradely transported from the intestine to the brain via the vagal nerve. However, it is not clear which machinery is involved in the transport of different α-synuclein forms, especially the aggregated ones (oligomers and fibrils), which likely contribute to pathology of PD [10, 34, 50]. As live-cell imaging would be technically challenging to perform in living animals, we used an in vitro system where cultured differentiated neuroblastoma cells (from the SH-SY5Y line), which exhibit neuronal morphology, were transfected with α-synuclein constructs expressing human α-synuclein tagged with full-length fluorescent protein (Venus) or co-transfected with Bimolecular Fluorescence Complementation (BiFC) truncated parts of a Venus, which upon dimerization and oligomerization of α-synuclein reveals fluorescence [15, 35]. Taking advantage of this system that allows us to visualize both total α-synuclein and specifically the aggregated α-synuclein with complemented fluorescence, we performed fluorescence recovery after photobleaching (FRAP) experiments in differentiated SH-SY5Y cells (Fig. 6a, b; Supplement Fig. 4). Functionality of axons in differentiated cells was validated by transfection using a mito-GFP construct visualizing active transport of mitochondria by live cell imaging (Supplement Movie).

To study the motility of aggregating α-synuclein, we first asked whether the transport of aggregated α-synuclein

in neurons occurs by an active process (protein–protein interaction) or by passive diffusion. We use two distinct models that represent these forms of transport, respectively. Cells, expressing full-length Venus alone (empty vector) or actin-GFP were used as controls. Venus alone, being a freely diffusing protein independent of molecular interactions, displayed a complete recovery of signal following photobleaching returning to the pre-bleach level ($p < 0.0001$) as expected. In contrast, we observed α-synuclein-Venus and the complemented α-synuclein-BiFC-Venus signal to recover only to 75 % of the pre-bleach intensity ($p < 0.0017$). Actin-GFP showed a much lower recovery ($p < 0.0002$), typical of a low motility protein dependent on protein–protein interaction. This was also expected, as actin has been documented to be primarily transported in SCb [4]. The rapid, but partial, recovery of complemented α-synuclein-BiFC-Venus suggests that it is involved in protein–protein interaction (Fig. 6b, c). As expected, similar results were seen for total α-synuclein-Venus.

Fast axonal transport is microtubule based, and microtubule itself is transported in SCa. To investigate whether transport of aggregated α-synuclein was microtubule dependent, we treated the cultures with 10 nM vinblastine, an agent known to destabilize microtubules [2, 20], for 1 h before the FRAP experiment. The treatment affected neither the protein mobility of actin-GFP nor that of Venus alone ($p = 0.1586$ and $p = 0.1618$, respectively). No increase in mobility was observed for α-synuclein-Venus reflecting the whole pool of protein regardless of being interacted to subcellular components or not (e.g., membrane bound, microtubule or soluble). The BiFC approach offers the unique opportunity to exclusively visualize the aggregating (oligomeric) form of α-synuclein. In this group, we observed a significant increase in mobility following treatment (Fig. 6d, $p = 0.00948$). The level of mobility of aggregated α-synuclein in vinblastine-treated cells was comparable to that of free diffusion, as seen in cells expressing Venus alone (Fig. 6d, $p = 0.64074$). This 25 % increase, for oligomeric α-synuclein, following vinblastine treatment shows that aggregated α-synuclein is directly interacting with microtubule in functional axons of neuron-like cells, suggesting aggregated α-synuclein is likely transported both by the fast component (microtubule based) as well as SCa and SCb.

Discussion

In the present study, we demonstrate that aggregated α-synuclein is transported from the intestine to the brain. Our in vitro data also suggest that aggregated α-synuclein is transported through both fast and slow axonal transports.

α-Synuclein and its aggregated forms are transported in long distance from the intestine to the brain

After intensive studies, Braak et al. [6–8] proposed the six stages of neuropathology during PD pathogenesis. The first sign of Lewy pathology appears in the projection neurons of the dorsal motor nucleus of the vagus at the early stage of PD [9]. Later on, the vulnerable brain regions are affected in a predictable sequence, progressing in a stereotypical caudal–rostral pattern starting in the lower brainstem, medulla oblongata, and exhibiting the pathology in more rostral regions later. A key question is how this stepwise temporal appearance is developed over time (over many years in humans). Braak hypothesized that the Lewy pathology retrogradely progresses from the intestine to the brain. However, some studies have argued against the findings of the Braak hypothesis, by showing non-stereotypic patterns of Lewy pathology [18, 37, 38]. In the present study, we provide direct evidence that retrogradely transported α-synuclein forms indeed lead to spread of the Lewy pathology from the peripheral tissue (gastrointestinal) to the brain via the vagal nerve. Similar phenomena are observed not only for monomeric α-synuclein, but also for oligomeric and fibrillar α-synuclein, the latter most likely being a significant contributor to the Lewy pathology propagation in PD conditions. The vagal route of α-synuclein transport has also been documented by systemic administration of the environmental toxin rotenone [36], as well as by directly injecting adeno-associated viral vectors overexpressing human α-synuclein into the vagal nerve [49]. The clear difference between the present study and previous work is that exogenous α-synuclein forms are not readily detected in the vagal nerves/neurons and the brain parenchyma [15, 31, 32, 49].

After being delivered to the gastrointestinal wall, α-synuclein must first be taken up into the vagal nerve terminals or indirectly to the enteric neurons and/or their terminals first, then trans-synaptically transfer via the synapses between the enteric neurons and the vagal nerves to reach the brain. Thus, the amount of transported α-synuclein is expected to be low. We found that all α-synuclein forms (monomers, oligomers and fibrils) are actively transported from the intestine to the dorsal motor nucleus of the vagus. It is, therefore, conceivable that the gut-to-brain route is an important route for α-synuclein propagation. The protein is taken up into the peripheral tissues and is transported to the lower brain. The spread of pathology is time dependent. Figure 6 illustrates the overview pattern of α-synuclein transport between the intestine and the brain. We readily observed distinct α-synuclein in the intestinal wall shortly (12 h) after injection, however, at the same time, we barely detected any α-synuclein in the vagal nerve, which became evident in the later time points. Correspondently, we did

not detect any human α-synuclein in the DMV 24 h after the injection while considerable numbers of α-synuclein-positive neurons were observed in the later time points (72–144 h) after the injection. Although, we did notice a stronger α-synuclein-positive signal in the DMV of animals injected with monomeric and oligomeric α-synuclein compared to those injected with fibrillar form or PD brain lysate, suggesting a difference in propensity to transport, we hesitate for such conclusions since transport most likely also depend on the success and favorable quality of injection sites in each animal. Several groups elegantly showed that α-synuclein pathology spread along the neuronal connections after injecting the PD brain lysate, transgenic mouse brain lysate or preformed α-synuclein fibrils in the striatum and the cortex of mice or monkeys [31, 32, 42, 43], where the exogenous α-synuclein induced a seeding effect of endogenous α-synuclein, suggesting a permissive templating prion-like process [16]. The time-dependent and connectivity-dependent spread of the Lewy pathology is closely accompanied by dopaminergic neuronal cell death at 90 and 180 days post-injection [31]. It is worth mentioning that we also examined potential cell death in the DMV with cell death markers, such as activated caspase 3, and α-synuclein presence in higher brain regions, such as the locus coeruleus and the substantia nigra (Fig. 7). We neither detect distinct dying cells, nor exogenous α-synuclein in these brain regions (data not shown). The discrepancy between our findings and theirs could be due to the dose of delivered α-synuclein and incubation time (6 days vs. 90–180 days) following injection.

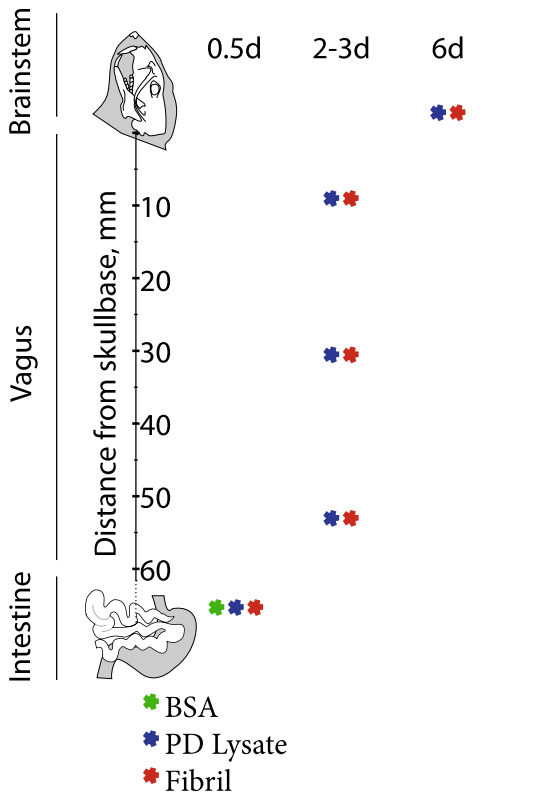

Fig. 7 An overview of uptake and transport of BSA and α-synuclein in the PD brain lysate or synthetic recombinant α-synuclein fibrils, in the intestines, along the vagal nerve and in the medulla oblongata, at different time points

The mechanisms of transport of α-synuclein species

Sufficient axonal transport is essential for neuronal function. Based on the speed of the trafficking, axonal transport is categorized into fast axonal transport (largely involved in membrane-bound organelles) with rates of 50–400 mm/day and slow axonal transports (SCa and SCb). SCa transports microtubules and neurofilaments at average rate of about 1 mm/day, while SCb transports handful soluble cytosolic proteins, including actin at average rate of about 2–8 mm/day [47]. Roy and his co-workers reported that α-synuclein was transported in SCb. It appeared that α-synuclein co-transported with other SCb proteins [44–46]. Using stop-flow/nerve crush operations and metabolic labeling of retinal ganglion cells, we demonstrated that (monomeric) α-synuclein is transported by all axonal transport components (fast transport, SCa and SCb) and that the majority of protein is transported through SCa and SCb, while one quarter is transported through fast axonal transport [19]. The oligomeric form of α-synuclein impairs microtubule–kinesin interaction and lead to early neurite pathology [41] and oligomeric and/or fibrillar α-synuclein is the vector of pathology propagation [1, 31, 42]. It is thus essential to understand the transport mechanism of oligomeric and fibrillar α-synuclein in neurons. In vitro studies with microfluidic chambers showed that preformed α-synuclein fibrils were not only taken up and transported within primary neurons but also transmitted to secondary neurons [13, 33]. Taking advantage of the unique strategy of BiFC, with the FRAP technique, we demonstrated that oligomeric α-synuclein and likely the fibrillar form as well, is directly associated with microtubule plausibly engaged in active transport. Likely, the aggregated forms of α-synuclein are involved in all form of axonal transports, as for monomeric α-synuclein by associating with fast transporting cargoes, interacting with microtubules and staying in soluble states. At certain conditions, such as phosphorylation or truncations, they may translocate from one subcellular compartment to another. Furthermore, we also demonstrated that assembled α-synuclein is retrogradely transported along long-distance ranges from the intestine to the brain. Given the fact that the full vagal nerve length is about 110–140 mm in adult rats from the DMV to the muscles in the intestine wall, our in vivo findings suggest an average translocation rate of 20–30 mm/day, i.e., faster

than SCb in the reported range of fast microtubule-associated transport [24], in support of multi-phasic transport. The actual transport rate is most likely faster as the estimated rate also covers the time required for accumulation of α-synuclein in the cell body in the DMV as well as time required for α-synuclein direct or indirect uptake into the axon of the projecting nerve cell. Because of the limitations of FRAP, specific membranous cargoes or transport motors that are involved in the transport of α-synuclein are yet to be evaluated.

The long-range anterograde and retrograde transport of α-synuclein assemblies may contribute to a complex spread of Lewy pathology. Numerous experimental evidences, including our present findings, support Braak's hypothesis that α-synuclein is transported retrogradely. Nonetheless, discrepant findings [18, 38] indicate diverse clinical features for PD with different subtypes of neuropathology. In an independent study, we recently demonstrated that aggregated α-synuclein is also transported anterogradely in neurons, for example, from the cortex to the spinal cord (Unpublished observations). The bidirectional transport of α-synuclein assemblies may account for the complexity of PD pathology.

Acknowledgments The authors wish to thank Marianne Juhlin and AnnaKarin Oldén for their excellent technical support. We thank Andrew C. McCourt for the linguistic revision of this manuscript. This work was funded by grants from the Swedish Research Council; Torsten Söderberg Foundation and Swedish Parkinson Foundation (J.-Y. L.). S.H., O.C., T.A., L.R. and J.-Y. L are active and supported by BAGADILICO—Excellence in Parkinson and Huntington Research, and the Strategic Research Area Multipark (Multidisciplinary research in Parkinson's disease at Lund University); L.B. and R.M. are supported by the Centre National de la Recherche Scientifique and Grants from the Agence Nationale de la Recherche (ANR-11-BSV8-021-01) and a 'Coup d'Elan a la Recherche Francaise' award from Fondation Bettencourt Schueller. Z.Y.W. and J.-Y.L. are supported by National Natural Science Foundation of China (81430025) and the Fundamental Research Funds for Central Universities of China (N130120002).

Conflict of interest The authors declare no competing financial interests.

References

1. Aguzzi A, Rajendran L (2009) The transcellular spread of cytosolic amyloids, prions, and prionoids. Neuron 64:783–790
2. Ahmad FJ, Echeverri CJ, Vallee RB, Baas PW (1998) Cytoplasmic dynein and dynactin are required for the transport of microtubules into the axon. J Cell Biol 140:391–401
3. Axelrod D, Koppel DE, Schlessinger J, Elson E, Webb WW (1976) Mobility measurement by analysis of fluorescence photobleaching recovery kinetics. Biophys J 16:1055–1069. doi:10.1016/S0006-3495(76)85755-4
4. Black MM, Lasek RJ (1979) Axonal transport of actin: slow component b is the principal source of actin for the axon. Brain Res 171:401–413
5. Braak H, de Vos RA, Bohl J, Del Tredici K (2006) Gastric alpha-synuclein immunoreactive inclusions in Meissner's and Auerbach's plexuses in cases staged for Parkinson's disease-related brain pathology. Neurosci Lett 396:67–72
6. Braak H, Del Tredici K (2009) Neuroanatomy and pathology of sporadic Parkinson's disease. Adv Anat Embryol Cell Biol 201:1–119
7. Braak H, Del Tredici K, Rub U, de Vos RA, Jansen Steur EN, Braak E (2003) Staging of brain pathology related to sporadic Parkinson's disease. Neurobiol Aging 24:197–211
8. Braak H, Ghebremedhin E, Rub U, Bratzke H, Del Tredici K (2004) Stages in the development of Parkinson's disease-related pathology. Cell Tissue Res 318:121–134
9. Braak H, Rub U, Gai WP, Del Tredici K (2003) Idiopathic Parkinson's disease: possible routes by which vulnerable neuronal types may be subject to neuroinvasion by an unknown pathogen. J Neural Transm 110:517–536
10. Danzer KM, Haasen D, Karow AR, Moussaud S, Habeck M, Giese A, Kretzschmar H, Hengerer B, Kostka M (2007) Different species of alpha-synuclein oligomers induce calcium influx and seeding. J Neurosci 27:9220–9232
11. Desplats P, Lee HJ, Bae EJ, Patrick C, Rockenstein E, Crews L, Spencer B, Masliah E, Lee SJ (2009) Inclusion formation and neuronal cell death through neuron-to-neuron transmission of alpha-synuclein. Proc Natl Acad Sci 106:13010–13015
12. Ellenberg J, Siggia ED, Moreira JE, Smith CL, Presley JF, Worman HJ, Lippincott-Schwartz J (1997) Nuclear membrane dynamics and reassembly in living cells: targeting of an inner nuclear membrane protein in interphase and mitosis. J Cell Biol 138:1193–1206
13. Freundt EC, Maynard N, Clancy EK, Roy S, Bousset L, Sourigues Y, Covert M, Melki R, Kirkegaard K, Brahic M (2012) Neuron-to-neuron transmission of alpha-synuclein fibrils through axonal transport. Ann Neurol 72:517–524. doi:10.1002/ana.23747
14. Ghee M, Melki R, Michot N, Mallet J (2005) PA700, the regulatory complex of the 26S proteasome, interferes with alpha-synuclein assembly. FEBS J 272:4023–4033
15. Hansen C, Angot E, Bergstrom AL, Steiner JA, Pieri L, Paul G, Outeiro TF, Melki R, Kallunki P, Fog K et al (2011) alpha-Synuclein propagates from mouse brain to grafted dopaminergic neurons and seeds aggregation in cultured human cells. J Clin Invest 121:715–725. doi:10.1172/JCI43366
16. Hardy J (2005) Expression of normal sequence pathogenic proteins for neurodegenerative disease contributes to disease risk: 'permissive templating' as a general mechanism underlying neurodegeneration. Biochem Soc Trans 33:578–581
17. Hawkes CH, Del Tredici K, Braak H (2009) Parkinson's disease: the dual hit theory revisited. Ann N Y Acad Sci 1170:615–622
18. Jellinger KA (2008) A critical reappraisal of current staging of Lewy-related pathology in human brain. Acta Neuropathol 116:1–16
19. Jensen PH, Li JY, Dahlstrom A, Dotti CG (1999) Axonal transport of synucleins is mediated by all rate components. Eur J Neurosci 11:3369–3376
20. Jordan MA, Wilson L (2004) Microtubules as a target for anticancer drugs. Nat Rev Cancer 4:253–265. doi:10.1038/nrc1317
21. Kordower JH, Chu Y, Hauser RA, Freeman TB, Olanow CW (2008) Lewy body-like pathology in long-term embryonic nigral transplants in Parkinson's disease. Nat Med 14:504–506
22. Kordower JH, Chu Y, Hauser RA, Olanow CW, Freeman TB (2008) Transplanted dopaminergic neurons develop PD pathologic changes: a second case report. Mov Disord 23:2303–2306
23. Kurowska Z, Englund E, Widner H, Lindvall O, Li J-Y, Brundin P (2011) Signs of degeneration in 12–22 year old grafts of

mesencephalic dopamine neurons in patients with Parkinson's disease. J Parkinsons Dis 1:83–92. doi:10.3233/jpd-2011-11004
24. Lasek RJ, Garner JA, Brady ST (1984) Axonal transport of the cytoplasmic matrix. J Cell Biol 99:212–221
25. Lebouvier T, Chaumette T, Paillusson S, Duyckaerts C, Bruley des Varannes S, Neunlist M, Derkinderen P (2009) The second brain and Parkinson's disease. Eur J Neurosci 30:735–741
26. Lee HJ, Suk JE, Lee KW, Park SH, Blumbergs PC, Gai WP, Lee SJ (2011) Transmission of synucleinopathies in the enteric nervous system of A53T alpha-synuclein transgenic mice. Exp Neurobiol 20:181–188. doi:10.5607/en.2011.20.4.181
27. Lee HJ, Suk JE, Patrick C, Bae EJ, Cho JH, Rho S, Hwang D, Masliah E, Lee SJ (2010) Direct transfer of alpha-synuclein from neuron to astroglia causes inflammatory responses in synucleinopathies. J Biol Chem 285:9262–9272
28. Lerner A, Bagic A (2008) Olfactory pathogenesis of idiopathic Parkinson disease revisited. Mov Disord 23:1076–1084
29. Li JY, Englund E, Holton JL, Soulet D, Hagell P, Lees AJ, Lashley T, Quinn NP, Rehncrona S, Bjorklund A et al (2008) Lewy bodies in grafted neurons in subjects with Parkinson's disease suggest host-to-graft disease propagation. Nat Med 14:501–503. doi:10.1038/nm1746
30. Li JY, Englund E, Widner H, Rehncrona S, Bjorklund A, Lindvall O, Brundin P (2010) Characterization of Lewy body pathology in 12- and 16-year-old intrastriatal mesencephalic grafts surviving in a patient with Parkinson's disease. Mov Disord 25:1091–1096. doi:10.1002/mds.23012
31. Luk KC, Kehm V, Carroll J, Zhang B, O'Brien P, Trojanowski JQ, Lee VM (2012) Pathological alpha-synuclein transmission initiates Parkinson-like neurodegeneration in nontransgenic mice. Science 338:949–953. doi:10.1126/science.1227157
32. Luk KC, Kehm VM, Zhang B, O'Brien P, Trojanowski JQ, Lee VM (2012) Intracerebral inoculation of pathological alpha-synuclein initiates a rapidly progressive neurodegenerative alpha-synucleinopathy in mice. J Exp Med 209:975–986. doi:10.1084/jem.20112457
33. Luk KC, Song C, O'Brien P, Stieber A, Branch JR, Brunden KR, Trojanowski JQ, Lee VM (2009) Exogenous {alpha}-synuclein fibrils seed the formation of Lewy body-like intracellular inclusions in cultured cells. Proc Natl Acad Sci 106:20051–20056
34. Nonaka T, Watanabe ST, Iwatsubo T, Hasegawa M (2010) Seeded aggregation and toxicity of {alpha}-synuclein and tau: cellular models of neurodegenerative diseases. J Biol Chem 285:34885–34898. doi:10.1074/jbc.M110.148460
35. Outeiro TF, Putcha P, Tetzlaff JE, Spoelgen R, Koker M, Carvalho F, Hyman BT, McLean PJ (2008) Formation of toxic oligomeric alpha-synuclein species in living cells. PLoS One 3:e1867
36. Pan-Montojo F, Schwarz M, Winkler C, Arnhold M, O'Sullivan GA, Pal A, Said J, Marsico G, Verbavatz JM, Rodrigo-Angulo M et al (2012) Environmental toxins trigger PD-like progression via increased alpha-synuclein release from enteric neurons in mice. Sci Rep 2:898. doi:10.1038/srep00898
37. Parkkinen L, Kauppinen T, Pirttila T, Autere JM, Alafuzoff I (2005) Alpha-synuclein pathology does not predict extrapyramidal symptoms or dementia. Ann Neurol 57:82–91
38. Parkkinen L, Pirttila T, Alafuzoff I (2008) Applicability of current staging/categorization of alpha-synuclein pathology and their clinical relevance. Acta Neuropathol 115(4):399–407
39. Phair RD, Gorski SA, Misteli T (2004) Measurement of dynamic protein binding to chromatin in vivo, using photobleaching microscopy. Methods Enzymol 375:393–414
40. Phillips RJ, Walter GC, Wilder SL, Baronowsky EA, Powley TL (2008) Alpha-synuclein-immunopositive myenteric neurons and vagal preganglionic terminals: autonomic pathway implicated in Parkinson's disease? Neuroscience 153:733–750
41. Prots I, Veber V, Brey S, Campioni S, Buder K, Riek R, Bohm KJ, Winner B (2013) alpha-Synuclein oligomers impair neuronal microtubule-kinesin interplay. J Biol Chem 288:21742–21754. doi:10.1074/jbc.M113.451815
42. Recasens A, Dehay B, Bove J, Carballo-Carbajal I, Dovero S, Perez-Villalba A, Fernagut PO, Blesa J, Parent A, Perier C et al (2014) Lewy body extracts from Parkinson disease brains trigger alpha-synuclein pathology and neurodegeneration in mice and monkeys. Ann Neurol 75:351–362. doi:10.1002/ana.24066
43. Rey NL, Petit GH, Bousset L, Melki R, Brundin P (2013) Transfer of human alpha-synuclein from the olfactory bulb to interconnected brain regions in mice. Acta Neuropathol 126:555–573. doi:10.1007/s00401-013-1160-3
44. Roy S, Winton MJ, Black MM, Trojanowski JQ, Lee VM (2008) Cytoskeletal requirements in axonal transport of slow component-b. J Neurosci 28:5248–5256
45. Roy S, Winton MJ, Black MM, Trojanowski JQ, Lee VM (2007) Rapid and intermittent cotransport of slow component-b proteins. J Neurosci 27:3131–3138
46. Scott DA, Das U, Tang Y, Roy S (2011) Mechanistic logic underlying the axonal transport of cytosolic proteins. Neuron 70:441–454. doi:10.1016/j.neuron.2011.03.022
47. Shea TB, Flanagan LA (2001) Kinesin, dynein and neurofilament transport. Trends Neurosci 24:644–648
48. Snapp EL, Altan N, Lippincott-Schwartz J (2003) Measuring protein mobility by photobleaching GFP chimeras in living cells. Curr Protoc Cell Biol. doi: 10.1002/0471143030.cb2101s19
49. Ulusoy A, Rusconi R, Perez-Revuelta BI, Musgrove RE, Helwig M, Winzen-Reichert B, Di Monte DA (2013) Caudo-rostral brain spreading of alpha-synuclein through vagal connections. EMBO Mol Med 5:1051–1059. doi:10.1002/emmm.201302475
50. Winner B, Jappelli R, Maji SK, Desplats PA, Boyer L, Aigner S, Hetzer C, Loher T, Vilar M, Campioni S et al (2011) In vivo demonstration that alpha-synuclein oligomers are toxic. Proc Natl Acad Sci 108:4194–4199. doi:10.1073/pnas.1100976108